

Cite this: *Dalton Trans.*, 2024, **53**, 11876

# Electron-rich pyridines with *para*-N-heterocyclic imine substituents: ligand properties and coordination to CO<sub>2</sub>, SO<sub>2</sub>, BCl<sub>3</sub> and Pd<sup>II</sup> complexes†

Jonas H. Franzen,<sup>a</sup> Lukas F. B. Wilm,<sup>b</sup> Philipp Rotering,<sup>a</sup> Klaus Wurst,<sup>a</sup> Michael Seidl<sup>a</sup> and Fabian Dielmann<sup>✉</sup>

Electron-rich pyridines with  $\pi$  donor groups at the *para* position play an important role as nucleophiles in organocatalysis, but their ligand properties and utilization in coordination chemistry have received little attention. Herein, we report the synthesis of two electron-rich pyridines **1** and **2** bearing N-heterocyclic imine groups at the *para* position and explore their coordination chemistry. Experimental and computational methods were used to assess the donor ability of the new pyridines showing that they are stronger donors than aminopyridines and guanidiny pyridines, and that the nature of the N-heterocyclic backbone has a strong influence on the pyridine donor strength. Coordination compounds with Lewis acids including the CO<sub>2</sub>, SO<sub>2</sub>, BCl<sub>3</sub> and Pd<sup>II</sup> ions were synthesized and characterized. Despite the ambident character of the new pyridines, coordination preferentially occurs at the pyridine-N atom. Methyl transfer experiments reveal that **1** and **2** can act as demethylation reagents.

Received 13th May 2024,  
Accepted 17th June 2024

DOI: 10.1039/d4dt01399a

rsc.li/dalton

## Introduction

Pyridines have been proved to be remarkably versatile synthetic building blocks and important tools in coordination chemistry and catalysis. The parent pyridine is a rather weak base and is therefore often incorporated into polydentate chelating ligands such as bipyridines and terpyridines. Donor-substituted, electron-rich pyridines, on the other hand, play an important role as nucleophilic organocatalysts for a number of synthetic transformations such as acylations,<sup>1–9</sup> esterifications<sup>10,11</sup> and silylations.<sup>12–14</sup> Zipse and coworkers calculated the methyl cation affinity (MCA) and proton affinity (PA) of a series of electron-rich pyridines and showed that the MCA is a useful descriptor for catalytic activity.<sup>15–18</sup> Pyridines with  $\pi$  donor substituents at the *para* position proved to be particularly active catalysts,<sup>1,4</sup> and 4-dimethylaminopyridine (DMAP) and 4-pyrrolidinopyridine (PPY) have been regarded as

benchmarks for decades (Fig. 1).<sup>1,2,19,20</sup> Later, annulated aminopyridines such as 9-azajulolidene<sup>21</sup> (**I**), 3,4-diaminopyridines<sup>15,22,23</sup> and 3,4,5-triaminopyridines,<sup>23,24</sup> including 4-guanidyl-substituted pyridines (**II**, **III**),<sup>3,25</sup> were found to outperform these benchmarks in acylation reactions. Phosphazeny-based pyridines (**IV**) are among the most active catalysts, but their use is limited due to the possible cleavage of the PN bond with the irreversible formation of phosphine oxides.<sup>26,27</sup> Apart from neutral pyridines, the incorporation of anionic groups leads to negatively charged pyridines (**V–VII**), which outperform DMAP in terms of their nucleophilicity and catalytic activity in the urethane-forming reaction.<sup>28–30</sup>

To date, the development of electron-rich pyridines has mainly been focused on their application in organocatalysis, while their properties as ligands in coordination chemistry have received little attention. The attempt to prepare transition

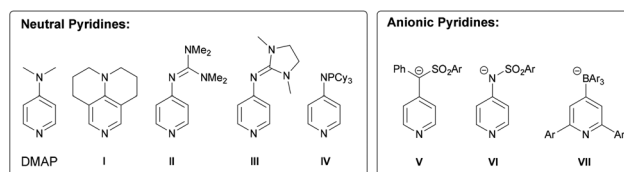


Fig. 1 Selected examples of neutral and anionic electron-rich pyridines.

<sup>a</sup>Institut für Allgemeine, Anorganische und Theoretische Chemie, Leopold-Franzens-Universität Innsbruck, Innrain 80-82, 6020 Innsbruck, Austria.

E-mail: fabian.dielmann@uibk.ac.at

<sup>b</sup>Institut für Anorganische und Analytische Chemie, Universität Münster  
Corrensstrasse 30, 48149 Münster, Germany

† Electronic supplementary information (ESI) available. CCDC 2354124–2354133. For ESI and crystallographic data in CIF or other electronic format see DOI: <https://doi.org/10.1039/d4dt01399a>



metal complexes with **VII** was unsuccessful due to single electron transfer processes from the electron-rich pyridine.<sup>31,32</sup> 2,3,5,6-Tetrakis(tetramethylguanidino)pyridine also readily undergoes electron transfer processes, yet Cu<sup>I</sup> complexes have been prepared. However, the complexation of the Cu<sup>I</sup> ions occurs *via* the guanidino rather than the pyridine donor atoms.<sup>33,34</sup> Terpyridines bearing dialkylamino groups were employed as ligands in homoleptic Ru<sup>II</sup>, Co<sup>II</sup>, Zn<sup>II</sup> and Fe<sup>II</sup> complexes.<sup>35,36</sup> The latter complex has recently been used as a catalyst in the electroreduction of CO<sub>2</sub>.<sup>37</sup>

We have shown that N-heterocyclic imines (NHIs)<sup>38,39</sup> are very effective substituents for generating highly electron-rich phosphines or porphyrins.<sup>40–46</sup> An attractive feature of NHIs is that variations in the backbone strongly affect the ability of the exocyclic N atom to act as a  $\pi$  donor, providing a tool for electronic fine-tuning without compromising steric properties.<sup>47</sup> Based on the molecular electrostatic potential (MESP)<sup>48–50</sup> topology analysis, Krishnapriya and Suresh recently indicated that NHI substituents are very effective at increasing the electron-density at the pyridine-N atom which leads to strong donor interactions with metal centers.<sup>51</sup> Here we report the synthesis of two electron-rich pyridines bearing different NHI groups at the *para* position (Fig. 2) and investigate their potential to act as strong donor ligands in coordination chemistry.

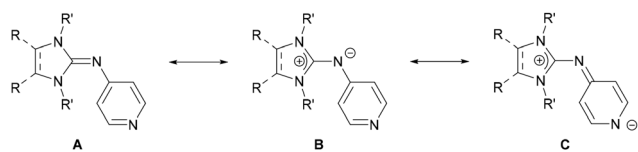


Fig. 2 Resonance structures of NHI-pyridines.

## Results and discussion

Pyridines **1** and **2** were synthesized according to the reported procedure for the synthesis of N-heterocyclic imines<sup>52,53</sup> *via* coupling of 4-aminopyridine and *N,N*-diisopropyl-4,5-dimethyl-2-chloroimidazolium tetrafluoroborate or *N,N*-di-*tert*-butyl-2-chloroimidazolium tetrafluoroborate, respectively (Fig. 3). The attempted synthesis of **1** in analogy to the preparation of **III**<sup>54</sup> using triethylamine as the base did not result in the selective formation of **1**. Instead, the disubstituted dication **3** was observed, as a result of the reaction of the aminopyridine with two equivalents of the imidazolium salt. Using a mixture of triethylamine and KF, **3** was formed selectively, and it was isolated after aqueous workup in 41% yield. To prevent the generation of the stable dication **3**, we opted to increase the electrophilicity of the azolium salt *via* the *in situ* generation of the corresponding fluoroazolium salts without using NEt<sub>3</sub> as an additional base. In fact, heating a suspension of 4-aminopyridine, the chloroazolium salt and KF in acetonitrile in a sealed vessel at 160 °C (**1**) or 90 °C (**2**) for three days led to the formation of **1** and **2**, which were isolated after extraction with hot *n*-hexane and recrystallization as white solids in good yield (Fig. 3). The pyridines **1** and **2** are benchtop-stable crystalline solids that are soluble in non-polar and polar organic solvents. No evidence of degradation was detected by <sup>1</sup>H NMR analysis after exposure of solid samples of **1** and **2** to atmospheric oxygen for several weeks. The pyridine <sup>1</sup>H NMR resonances of **1** (7.84 and 6.17 ppm) are shielded compared to those of **2** (8.49 and 6.50 ppm) indicating that the pyridine ring is more electron-rich in the case of **1** which agrees with the stronger  $\pi$  donor ability of the corresponding NHI substituent.<sup>38,42,53</sup> The solid-state structures of **1**, **2** and the dication **3** were established from single-crystal X-ray diffraction (SCXRD) studies (Fig. 3). As a common structural feature, the

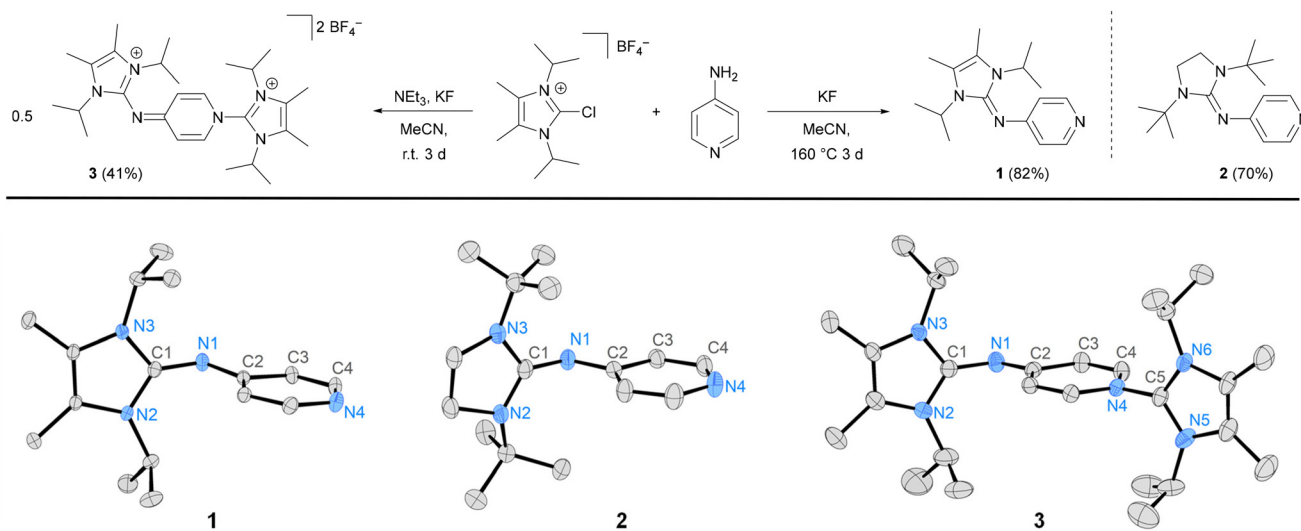


Fig. 3 Synthesis of pyridines **1**, **2** and the dication **3**. Molecular structures of **1**, **2**, and **3** with ellipsoids set at 50% probability. Hydrogen atoms and counter anions are omitted for clarity. Selected structural parameters of **1**, **2** and **3** are listed in Table 1.

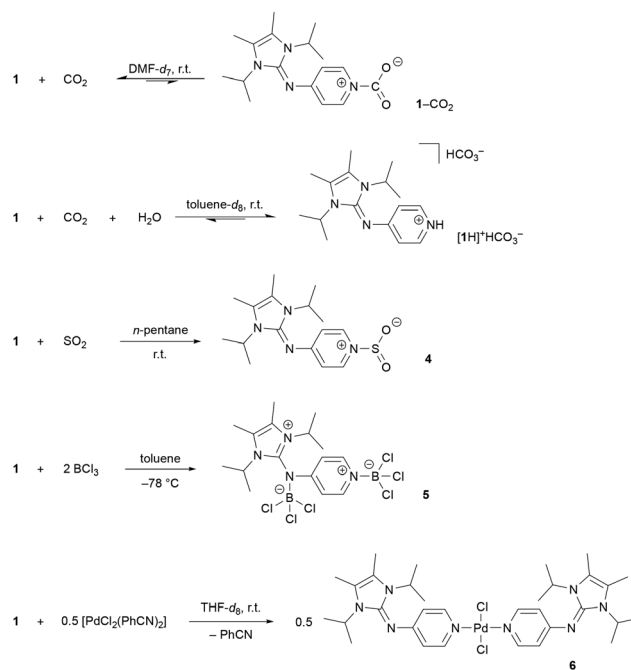


imidazole rings are nearly orthogonal to the pyridine ring (angle between the imidazole plane and pyridine plane for **1**: 82.1°, **2**: 87.1°, **3**: 82.1°) and the C1–N1–C2 bond angles are in a similar range (**1**: 123.21°, **2**: 124.52°, **3**: 126.82°). As expected for conjugated  $\pi$  systems, the C–N bond distances (1.317–1.361 Å) are in between those of classical C–N single and C=N double bonds (*cf.* Table 1).<sup>55,56</sup>

The reactivity of **1** towards the Lewis acids CO<sub>2</sub>, SO<sub>2</sub>, BCl<sub>3</sub> and Pd<sup>II</sup> complexes was investigated to determine which nitrogen donor site binds preferentially to Lewis acids and to rank the ligand donor strength. The interaction of pyridine with CO<sub>2</sub> has been thoroughly studied due to its relevance in the context of CO<sub>2</sub> conversion. While unsubstituted pyridine is not basic enough to form isolable adducts with CO<sub>2</sub>,<sup>57,58</sup> spectroscopic evidence exists for the carbamate radical anion, which is the reduced form and has been proposed as a key intermediate in (photo)electrocatalytic CO<sub>2</sub> reduction processes.<sup>59–61</sup> We, therefore, were curious if the interaction between the electron-rich pyridine **1** and CO<sub>2</sub> would be detectable. Subjecting an anhydrous toluene-*d*<sub>8</sub> solution of **1** to an atmosphere of 0.8 bar of <sup>13</sup>CO<sub>2</sub> did not lead to the precipitation of the corresponding CO<sub>2</sub> adduct, although CO<sub>2</sub> complexes were isolated for NHIs with alkyl groups at the exocyclic nitrogen atom.<sup>53</sup> Furthermore, the NMR analysis of the toluene solution gave no evidence of an interaction of **1** with CO<sub>2</sub> at room temperature. Since polar solvents were shown to stabilize zwitterionic CO<sub>2</sub> adducts,<sup>53,62</sup> the experiment was repeated using anhydrous DMF-*d*<sub>7</sub> and a higher CO<sub>2</sub> pressure. Indeed, the <sup>1</sup>H and <sup>13</sup>C NMR resonances of **1** shift upon pressurizing the DMF-*d*<sub>7</sub> solution with 4 bar CO<sub>2</sub>. Further evidence for the presence of the short-lived **1**–CO<sub>2</sub> complex in solution was provided by a variable temperature NMR study showing characteristic deshielding of the pyridine resonances in the <sup>1</sup>H NMR spectra (see the ESI and Fig. S20† for details). It should be noted that this is the first spectroscopic evidence of a pyridine–CO<sub>2</sub> complex. To study how water influences the reaction of **1** with CO<sub>2</sub>, a toluene solution containing **1** and stoichiometric amounts of water was pressurized with 4 bar CO<sub>2</sub>, which resulted in the immediate formation of the bicarbonate salt [1H]<sup>+</sup>HCO<sub>3</sub><sup>–</sup> as a voluminous white precipitate. The same behavior is observed for tertiary amines which are important sorbents in the context of CO<sub>2</sub> capture,<sup>63</sup> while pyridine is not basic enough for such CO<sub>2</sub> capture reactions. Without a CO<sub>2</sub> atmosphere,

the bicarbonate salt [1H]<sup>+</sup>HCO<sub>3</sub><sup>–</sup> decomposes slowly at ambient temperature into **1**, water and CO<sub>2</sub> (Scheme 1). Pressurizing **1** and 1.5 eq. of water in the more polar solvent DMF-*d*<sub>7</sub> with 4 bar CO<sub>2</sub> led to the broadening and shifting of the H<sub>2</sub>O resonance in the <sup>1</sup>H NMR spectrum. In addition, the CO<sub>2</sub> resonance is broadened in the <sup>13</sup>C NMR spectrum. Both indicate the reversible formation of [1H]<sup>+</sup>HCO<sub>3</sub><sup>–</sup> in DMF solution (see the ESI and Fig. S16 and S17† for details). Collectively, these experiments indicate that **1** forms reversible complexes with CO<sub>2</sub> *via* low energy barrier processes, which makes it a promising nucleophile for CO<sub>2</sub> activation protocols.<sup>64–66</sup>

SO<sub>2</sub> is more acidic than CO<sub>2</sub> and the formation of the pyridine adduct therefore is energetically favored by  $\Delta G = -0.82$  kcal mol<sup>–1</sup> in CCl<sub>4</sub>.<sup>67</sup> While the SO<sub>2</sub> adduct of the unsubstituted pyridine is not isolable, the more basic DMAP forms a room temperature stable SO<sub>2</sub> adduct.<sup>68</sup> Pressurizing a



**Scheme 1** Synthesis of compounds **4**–**6** and formation of the **1**–CO<sub>2</sub> adduct and the bicarbonate salt [1H]<sup>+</sup>HCO<sub>3</sub><sup>–</sup>.

**Table 1** Selected bond lengths [Å] and angles [°] of the NHI-pyridine moiety in the solid-state structures of **1**, **2**, **3**, **4**, **5**, **6**, **7** and **8**

	<b>1</b>	<b>2</b>	<b>3</b>	<b>4</b>	<b>5</b>	<b>6</b>	<b>7</b>	<b>8</b>
C1–N1	1.337(2)	1.328(2)	1.377(5)	1.347(2)	1.394(2)	1.339(3)	1.353(3)	1.324(4)
C1–N2	1.367(2)	1.361(2)	1.337(5)	1.355(2)	1.339(2)	1.353(3)	1.353(3)	1.361(4)
C1–N3	1.357(2)	1.359(2)	1.342(4)	1.352(2)	1.339(2)	1.364(3)	1.357(3)	1.354(4)
C2–N1	1.348(2)	1.344(2)	1.317(4)	1.339(2)	1.381(3)	1.349(3)	1.347(3)	1.334(4)
C2–C3	1.416(2)	1.412(2)	1.431(5)	1.426(2)	1.413(3)	1.420(3)	1.416(3)	1.414(4)
C3–C4	1.377(2)	1.374(2)	1.347(5)	1.365(2)	1.367(4)	1.360(3)	1.372(3)	1.372(4)
C4–N4	1.343(2)	1.342(2)	1.378(4)	1.350(2)	1.356(3)	1.353(3)	1.352(3)	1.348(4)
N1–C1–N2	127.6(1)	124.9(1)	126.8(3)	126.5(2)	125.3(9)	122.7(2)	124.7(2)	125.0(3)
C1–N1–C2	123.2(2)	124.5(1)	119.2(3)	121.2(2)	116.4(2)	122.2(2)	119.4(2)	129.5(3)
N2–C1–N1–C2	77.5(2)	84.8(2)	87.9(5)	76.6(2)	89.8(2)	58.2(2)	62.6(2)	86.3(4)



solution of **1** in *n*-pentane with 2 bar SO<sub>2</sub> led to the immediate precipitation of the SO<sub>2</sub> adduct **4** as a light-yellow solid in quantitative yield. The pyridine <sup>1</sup>H resonances get deshielded upon SO<sub>2</sub> complexation (**4**: 7.95 ppm, 6.39 ppm; **1**: 7.84 ppm, 6.17 ppm). An SCXRD study confirmed that SO<sub>2</sub> is bound to the pyridine nitrogen atom (Fig. 4). The S atom is in a trigonal-pyramidal coordination environment with an N–S bond length of 1.983 Å, an average S–O bond length of 1.421 Å and an O–S–O bond angle of 116.5°. As expected, the structural parameters of the SO<sub>2</sub> moiety of **4** and of the DMAP-SO<sub>2</sub> adduct (S–N: 1.991 Å, S–O: 1.446 Å, O–S–O: 114.75°)<sup>68</sup> are very similar. It is noteworthy that despite the excess SO<sub>2</sub> used in the reaction, only one molecule of SO<sub>2</sub> is coordinated by the pyridine moiety, suggesting a significant basicity difference between the two nitrogen donor atoms of **1**. Consistent with this regioselectivity, calculations on a benzimidazolin-2-ylidenamino pyridine show that the MCA of the pyridine-N is more exothermic by 15.71 kcal mol<sup>-1</sup> than that of the imino-N atom.<sup>69</sup>

Pyridine **1** was therefore reacted with the strong Lewis acid BCl<sub>3</sub> to investigate whether both nitrogen donor sites are available for coordination. Addition of BCl<sub>3</sub> to a toluene solution of **1** at -78 °C led to the precipitation of **5** as a white solid (Scheme 1), which was isolated in low yield by filtration. The adduct **5** is sparingly soluble in polar solvents like DCM and fluorobenzene. Coordination of the imino-N atom to the bulky BCl<sub>3</sub> moiety hampers rotation around the exocyclic C–N bond in **5**, as indicated by the two doublets in the <sup>1</sup>H NMR spectrum at 1.53 ppm and 1.40 ppm of the diastereotopic CH<sub>3</sub> groups. Moreover, the pyridine <sup>1</sup>H resonances are significantly deshielded (**5**: 8.92 ppm, 7.45 ppm; **1**: 7.84 ppm, 6.17 ppm). The <sup>11</sup>B NMR spectrum shows two singlets at 7.7 ppm and 5.8 ppm in the range of the resonance of the pyridine-BCl<sub>3</sub> adduct (δ = 8.1 ppm).<sup>70</sup> The solid-state structure of **5** was established from an SCXRD study confirming the ambident character of the NHI-substituted pyridine (Fig. 4). Both boron atoms are in a tetrahedral coordination environment and exhibit

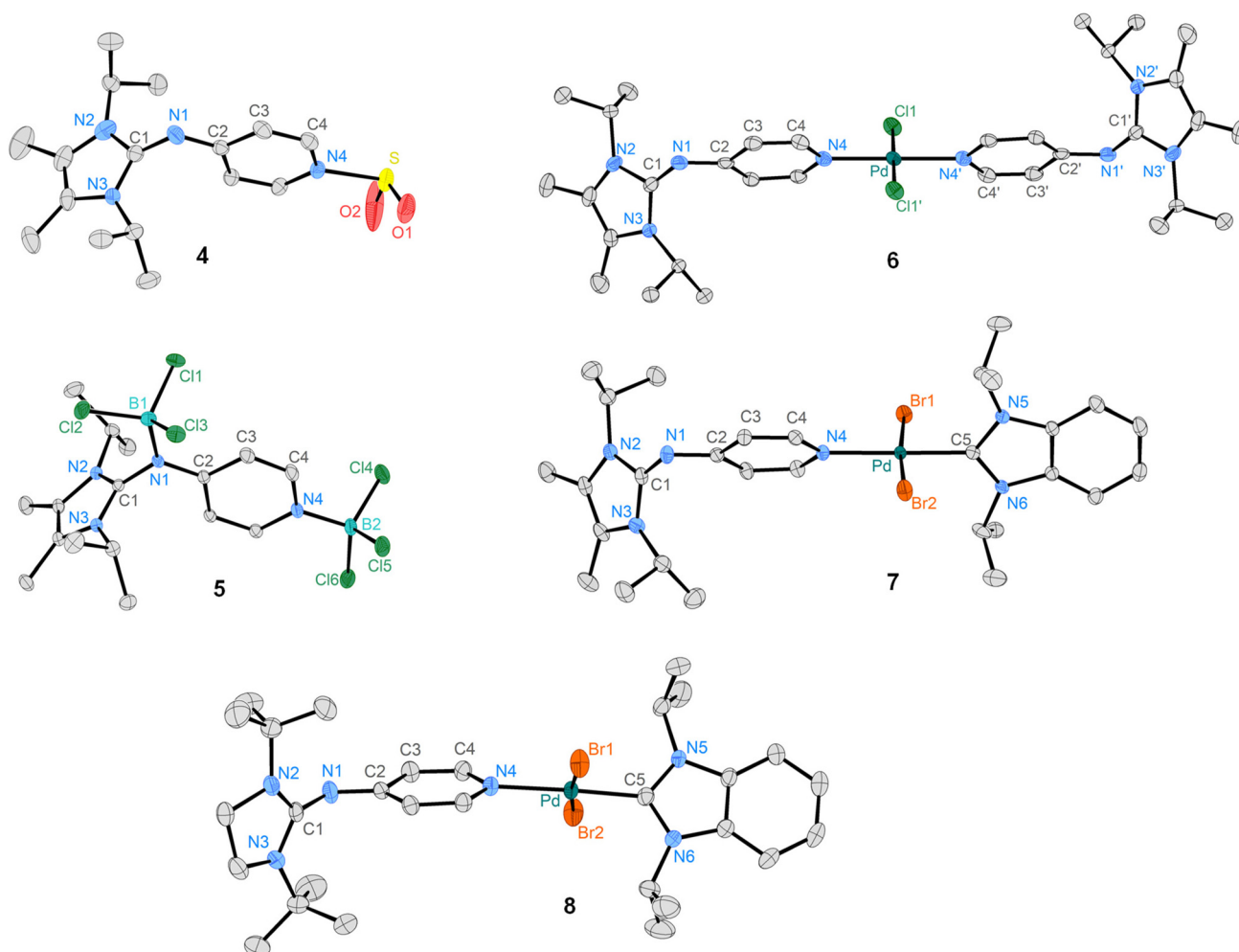


**Fig. 4** Molecular structures of compounds **4**–**8** with ellipsoids set at 50% probability. Hydrogen atoms are omitted for clarity. Selected bond lengths [Å] and angles [°]: **4**: N4–S 1.9826(13), S–O1 1.423(2), S–O2 1.418(2), O1–S–O2 116.47(11); **5**: N1–B1 1.541(3), N4–B2 1.583(3); ∠ B1–C1 1.859, ∠ B2–C1 1.843; **6**: Pd–N4 2.023(2), Pd–Cl1 2.3061(5), Cl1–Pd–N4 89.56(2); **7**: Pd–N4 2.088(2), Pd–C5 1.954(2), Pd–Br1 2.423(3), Br1–Pd–N4 92.55(5); **8**: Pd–N4 2.101(2), Pd–C5 1.958(3), Pd–Br1 2.436(4), N4–Pd–Br1 93.17(7).



shorter N–B bond lengths (N1–B1: 1.541 Å, N4–B2: 1.583 Å) than Me<sub>3</sub>N–BCl<sub>3</sub> (1.610 Å).<sup>71</sup> We next explored the formation of Pd<sup>II</sup> complexes with electron-rich pyridines. Treatment of [PdCl<sub>2</sub>(PhCN)<sub>2</sub>] with two equivalents of **1** in THF led to the selective formation of complex *trans*-[PdCl<sub>2</sub>(**1**)<sub>2</sub>] (**6**), which was obtained as an air-stable yellow solid in quantitative yield (Scheme 1). The solid-state structure of **6** displays a square planar geometry at Pd<sup>II</sup> with the pyridine ligands in the *trans* position (Fig. 4). The selective formation of the pyridine-bound Pd<sup>II</sup> complex **6** prompted us to assess the donor strength of **1** and **2** using the Huynh Electronic Parameter (HEP).<sup>72–74</sup> This method utilizes the <sup>13</sup>C NMR chemical shift of the carbene C atom in complexes *trans*-[PdBr<sub>2</sub>(BiPr)(L)] (BiPr = 1,3-dimethylbenzimidazolin-2-ylidene) as a probe to determine the donor strength of the ligand L. Treatment of **1** and **2** with the Pd<sup>II</sup> dimer [PdBr<sub>2</sub>(BiPr)]<sub>2</sub> cleanly gave the corresponding complexes *trans*-[PdBr<sub>2</sub>(BiPr)(**1**)] (**7**) and *trans*-[PdBr<sub>2</sub>(BiPr)(**2**)] (**8**) (*vide supra*). The <sup>1</sup>H NMR spectra of **7** and **8** show one set of signals for the pyridine ligands. The methyl resonances of the iPr groups of **1** are magnetically equivalent, consistent with coordination of the pyridine-N atom to the Pd<sup>II</sup> center. SCXRD studies confirm the *trans* arrangement of the pyridine ligands with Pd1–N4 bond lengths of 2.088 Å (**7**) and 2.101 Å (**8**), that are slightly elongated compared to that of **6** (2.023 Å). The <sup>13</sup>C resonance of the carbene C atom was detected at 163.2 ppm (**7**) and 163.1 ppm (**8**), which suggests that **1** and **2** are stronger donors than pyridine (160.0 ppm)<sup>72</sup> and DMAP (161.9 ppm)<sup>75</sup> (Fig. 5). The TEP values calculated using the method reported by Gusev<sup>76</sup> show the same trend (**1**: 2061.28 cm<sup>-1</sup>, **2**: 2062.52 cm<sup>-1</sup>, DMAP: 2065.42 cm<sup>-1</sup>).

Collectively, these results show that the introduction of NHI substituents at the *para* position is more effective than dialkylamino groups in increasing the donor properties of pyridine. The TEP and HEP both take the σ and π contributions of the ligand into account for ranking the donor strength. To gauge the σ donor ability of **1** and **2**, we therefore calculated the methyl cation affinities (MCA) using the method of Zipse and coworkers.<sup>16,35,77</sup> Comparison of the MCA of **1** and **2** with other substituted pyridines gives the same qualitative trend as

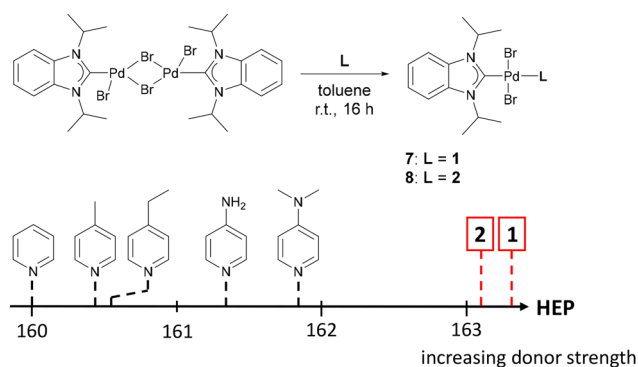


**Fig. 5** The Huynh electronic parameter (HEP) scale for different pyridines. The chemical shifts of the <sup>13</sup>C(<sup>1</sup>H) carbene resonance of the BiPr ligand are listed in Table 2.

**Table 2** Methyl cation affinity (MCA) and Huynh electronic parameter (HEP) of different pyridines. MCA values were calculated at the MP2(FC)/6-31+G(2d,p)//B98/6-31G(d) level of theory

Lewis base (LB)	MCA (kJ mol <sup>-1</sup> )	δ C <sub>carbene</sub> <sup>a</sup> (ppm)
Pyridine	518.7 <sup>b</sup>	160.1 <sup>c</sup>
4-Picoline	532.8 <sup>b</sup>	160.4 <sup>d</sup>
4-Ethylpyridine	—	160.5 <sup>d</sup>
4-Aminopyridine	—	161.3 <sup>d</sup>
DMAP	581.2 <sup>b</sup>	161.9 <sup>d</sup>
4-Tmg-pyridine(n)	597.5 <sup>b</sup>	—
9-Azajulolidene(t)	602.4 <sup>b</sup>	—
DBN	611.3 <sup>b</sup>	—
<b>1</b>	659.2	163.2
<b>2</b>	624.8	163.1

<sup>a</sup> Measured in CDCl<sub>3</sub> and internally referenced to the solvent residual signal at 77.7 ppm relative to TMS. <sup>b</sup> Ref. 16 <sup>c</sup> Ref. 74 <sup>d</sup> Ref. 75

observed for the HEP and TEP (Table 2). Notably, **1** and **2** both have considerably higher MCA than the acyclic guanidine derivative **II** and the organic superbases DBN (1,5-diazabicyclo(4.3.0)non-5-en).

The large differences in the calculated MCA inspired us to experimentally investigate the transfer of methyl groups between pyridine derivatives (Scheme 2). Several methodologies have been reported for the N-dealkylation of pyridinium salts,<sup>78</sup> which typically involve heating of the salt in the presence of a base including pyridine,<sup>79</sup> N-methylimidazole and triphenylphosphine.<sup>80</sup> In the case of pyridinium iodide salts, the demethylation was shown to be a two-step process.<sup>81,82</sup> The first and rate-determining step involves an S<sub>N</sub>2 substitution with the iodide counter anion acting as the nucleophile to generate pyridine and iodomethane. The second and faster step is the subsequent methylation of the sequestration reagent with the liberated iodomethane. We studied the methyl cation transfer by heating MeCN-*d*<sub>3</sub> solutions containing stoichiometric mixtures of **1** and the methyl-



Lewis base (LB)	MCA / kJ·mol <sup>-1</sup>	Yield
pyridine	518.7 <sup>a</sup>	99%
4-picoline	532.8 <sup>a</sup>	93%
DMAP	581.2 <sup>a</sup>	15%
<b>2</b>	624.8	0%



Lewis base (LB)	MCA / kJ·mol <sup>-1</sup>	Yield
pyridine	518.7 <sup>a</sup>	99%
4-picoline	532.8 <sup>a</sup>	95%

**Scheme 2** Methyl cation transfer experiments using **1** (top) and DMAP (bottom) as a sequestration reagent. NMR yields after heating the MeCN-*d*<sub>3</sub> solutions in sealed NMR tubes at 160 °C for 7 days. <sup>a</sup>ref. 16



ated pyridinium iodide salts in sealed NMR tubes. The reaction process was monitored by  $^1\text{H}$  NMR spectroscopy. This showed that prolonged heating of the reaction mixture to 160 °C was required to achieve appreciable transfer rates. Demethylation of the pyridinium and 4-picolinium salts takes place in high yields using **1** or DMAP as a methyl scavenger. **1** and DMAP show similar reaction rates (see the ESI† for details), which agrees with the abovementioned two-step mechanism in which the iodine counterion is the active demethylation agent. Accordingly, methyl transfer from the  $[\text{DMAP}\cdot\text{Me}]^+\text{I}^-$  salt to **1** is very slow with only 15% conversion after one week, and no sign of demethylation was detected in the case of  $[\text{2-Me}]^+\text{I}^-$ . The rate of methyl transfer thus depends primarily on the MCA of the methylated base and is independent of the  $\Delta\text{MCA}$  between the bases in the reaction mixture.

## Conclusion

In conclusion, we find that pyridines bearing N-heterocyclic imine substituents at the *para* position, which so far have only been examined with respect to their catalytic potential in acylation reactions of alcohols, show promise as strong donor ligands in coordination chemistry. The experimental determination of the HEP and the calculation of the TEP and MCA show that pyridines **1** and **2** are considerably stronger donor ligands than the aminopyridine DMAP or the acyclic 4-guanidiny pyridine **II**. The descriptors indicate that the  $\pi$  donor ability of the N-heterocyclic imine substituent has a significant impact on the electronic properties of the pyridine, which provides leverage for tuning the stereoelectronic properties of pyridines. Reactivity studies with various Lewis acids show that **1** can act as an ambident ligand, with the pyridine nitrogen atom being preferentially coordinated. In addition, the transfer of methyl groups between different pyridines was investigated. This showed that **1** and DMAP can be used for the demethylation of pyridine derivatives at rates that depend primarily on the MCA of the latter. Furthermore, NHI-substituted pyridine derivatives are currently being developed in our laboratories with a focus on applications for small molecule activation and catalysis.

## Data availability

The data supporting this article have been included as part of the ESI.†

## Author contributions

J. H. F. and L. F. B. W. carried out experiments for the synthesis of **1** and **2** and their respective  $\text{Pd}^{\text{II}}$  complexes and Lewis acid adducts **4–8**. J. H. F. investigated the  $\text{CO}_2$  adduct formation and methyl cation transfer reactions. P. R. performed the calculations of the MCA and TEP values for **1** and **2**. L. F. B. W., K. W. and M. S. performed the SCXRD

studies. F. D. directed the investigations. The manuscript was written and edited by J. H. F. and F. D. with contributions from L. F. B. W. All authors have given approval to the final version of the manuscript.

## Conflicts of interest

There are no conflicts to declare.

## Acknowledgements

We sincerely thank the Tiroler Wissenschaftsförderung (TWF, F.45075) for funding to realize this project and to the German Academic Scholarship Foundation for a PhD fellowship (L. F. B. W.). We thank assoc. Prof. Dr Christoph Kreutz for the measurements of the variable temperature NMR spectra.

## References

- W. Steglich and G. Höfle, *Angew. Chem., Int. Ed. Engl.*, 1969, **8**, 981, (*Angew. Chem.*, 1969, **81**, 1001).
- G. Höfle, W. Steglich and H. Vorbrüggen, *Angew. Chem., Int. Ed. Engl.*, 1978, **17**, 569–583, (*Angew. Chem.*, 1978, **90**, 602–615).
- A. Hassner, L. R. Krepski and V. Alexanian, *Tetrahedron*, 1978, **34**, 2069–2076.
- A. C. Spivey and S. Arseniyadis, *Angew. Chem., Int. Ed.*, 2004, **43**, 5436–5441.
- E. F. V. Scriven, *Chem. Soc. Rev.*, 1983, **12**, 129.
- Applications of Dialkylaminopyridine (DMAP) Catalysts in Organic Synthesis*, ed. M. Ramiah and E. F. V. Scriven, 2003.
- G. C. Fu, *Acc. Chem. Res.*, 2000, **33**, 412–420.
- G. C. Fu, *Acc. Chem. Res.*, 2004, **37**, 542–547.
- U. Ragnarsson and L. Grehn, *Acc. Chem. Res.*, 1998, **31**, 494–501.
- L. J. Gooßen and A. Döhring, *Synlett*, 2004, 263–266.
- I. Held, P. von den Hoff, D. S. Stephenson and H. Zipse, *Adv. Synth. Catal.*, 2008, **350**, 1891–1900.
- S. K. Chaudhary and O. Hernandez, *Tetrahedron Lett.*, 1979, **20**, 99–102.
- P. Patschinski, C. Zhang and H. Zipse, *J. Org. Chem.*, 2014, **79**, 8348–8357.
- M. Marin-Luna, P. Patschinski and H. Zipse, *Chem. – Eur. J.*, 2018, **24**, 15052–15058.
- E. Larionov, F. Achraimer, J. Humin and H. Zipse, *ChemCatChem*, 2012, **4**, 559–566.
- Y. Wei, G. N. Sastry and H. Zipse, *J. Am. Chem. Soc.*, 2008, **130**, 3473–3477.
- C. Lindner, R. Tandon, B. Maryasin, E. Larionov and H. Zipse, *Beilstein J. Org. Chem.*, 2012, **8**, 1406–1442.
- I. Despotović and R. Vianello, *Chem. Commun.*, 2014, **50**, 10941–10944.
- N. de Rycke, F. Couty and O. R. P. David, *Chem. – Eur. J.*, 2011, **17**, 12852–12871.



- 20 M. Baidya and H. Mayr, *Chem. Commun.*, 2008, 1792–1794.
- 21 M. R. Heinrich, H. S. Klisa, H. Mayr, W. Steglich and H. Zipse, *Angew. Chem., Int. Ed.*, 2003, **42**, 4826–4828.
- 22 I. Held, S. Xu and H. Zipse, *Synthesis*, 2007, 1185–1196.
- 23 S. Singh, G. Das, O. V. Singh and H. Han, *Org. Lett.*, 2007, **9**, 401–404.
- 24 R. Tandon, T. Unzner, T. A. Nigst, N. de Rycke, P. Mayer, B. Wendt, O. R. P. David and H. Zipse, *Chem. – Eur. J.*, 2013, **19**, 6435–6442.
- 25 I. Held, E. Larionov, C. Bozler, F. Wagner and H. Zipse, *Synthesis*, 2009, 2267–2277.
- 26 N. A. Richard, C. K. Khor, S. M. Hetherington, S. L. Mills, A. Decken and C. A. Dyker, *Chem. – Eur. J.*, 2020, **26**, 17371–17375.
- 27 N. A. Richard, G. D. Charlton and C. A. Dyker, *Org. Biomol. Chem.*, 2021, **19**, 9167–9171.
- 28 E. Anders, U. Korn and A. Stankowiak, *Chem. Ber.*, 1989, **122**, 105–111.
- 29 J. Helberg, T. Ampßler and H. Zipse, *Chem. Commun.*, 2020, **85**, 5390–5402.
- 30 S. H. Dempsey, A. Lovstedt and S. R. Kass, *J. Org. Chem.*, 2023, **88**, 10525–10538.
- 31 N. M. C. Schmidlin, M. Lökov, I. Leito and T. Böttcher, *Chem. – Eur. J.*, 2018, **24**, 16851–16856.
- 32 N. M. C. Schmidlin, V. Radtke, A. Schmidt, M. Lökov, I. Leito and T. Böttcher, *Z. Anorg. Allg. Chem.*, 2022, **648**, e202200136.
- 33 S. Stang, A. Lebkücher, P. Walter, E. Kaifer and H.-J. Himmel, *Eur. J. Inorg. Chem.*, 2012, **2012**, 4833–4845.
- 34 S. Wiesner, A. Wagner, O. Hübner, E. Kaifer and H.-J. Himmel, *Chem. – Eur. J.*, 2015, **21**, 16494–16503.
- 35 P. Hommes, C. Fischer, C. Lindner, H. Zipse and H.-U. Reissig, *Angew. Chem., Int. Ed.*, 2014, **53**, 7647–7651.
- 36 M. Kleoff, S. Suhr, B. Sarkar, R. Zimmer, H.-U. Reissig, M. Marin-Luna and H. Zipse, *Chem. – Eur. J.*, 2019, **25**, 7526–7533.
- 37 S. Suhr, N. Schröter, M. Kleoff, N. Neuman, D. Hunger, R. Walter, C. Lücke, F. Stein, S. Demeshko, H. Liu, H.-U. Reissig, J. van Slageren and B. Sarkar, *Inorg. Chem.*, 2023, **62**, 6375–6386.
- 38 X. Wu and M. Tamm, *Coord. Chem. Rev.*, 2014, **260**, 116–138.
- 39 T. Ochiai, D. Franz and S. Inoue, *Chem. Soc. Rev.*, 2016, **45**, 6327–6344.
- 40 M. A. Wünsche, P. Mehlmann, T. Witteler, F. Buß, P. Rathmann and F. Dielmann, *Angew. Chem., Int. Ed.*, 2015, **54**, 11857–11860.
- 41 P. Mehlmann, C. Mück-Lichtenfeld, T. T. Y. Tan and F. Dielmann, *Chem. – Eur. J.*, 2017, **23**, 5929–5933.
- 42 T. Witteler, H. Darmandeh, P. Mehlmann and F. Dielmann, *Organometallics*, 2018, **37**, 3064–3072.
- 43 L. F. Wilm, P. Mehlmann, F. Buß and F. Dielmann, *J. Organomet. Chem.*, 2020, **909**, 121097.
- 44 M. D. Böhme, T. Eder, M. B. Röthel, P. D. Dutschke, L. F. B. Wilm, F. E. Hahn and F. Dielmann, *Angew. Chem., Int. Ed.*, 2022, **61**, e202202190, (*Angew. Chem.*, 2022, **134**, e202202190).
- 45 P. Roterling, L. F. B. Wilm, J. A. Werra and F. Dielmann, *Chem. – Eur. J.*, 2020, **26**, 406–411.
- 46 M. Abdinejad, L. F. B. Wilm, F. Dielmann and H. B. Kraatz, *ACS Sustainable Chem. Eng.*, 2021, **9**, 521–530.
- 47 P. Mehlmann, T. Witteler, L. F. B. Wilm and F. Dielmann, *Nat. Chem.*, 2019, **11**, 1139–1143.
- 48 C. H. Suresh and S. R. Gadre, *J. Am. Chem. Soc.*, 1998, **120**, 7049–7055.
- 49 G. S. Remya and C. H. Suresh, *Phys. Chem. Chem. Phys.*, 2016, **18**, 20615–20626.
- 50 F. B. Sayyed and C. H. Suresh, *Tetrahedron Lett.*, 2009, **50**, 7351–7354.
- 51 V. U. Krishnapriya and C. H. Suresh, *Organometallics*, 2023, **42**, 571–580.
- 52 R. A. Kunetskiy, S. M. Polyakova, J. Vavřík, I. Císařová, J. Saame, E. R. Nerut, I. Koppel, I. A. Koppel, A. Kütt, I. Leito and I. M. Lyapkalo, *Chem. – Eur. J.*, 2012, **18**, 3621–3630.
- 53 L. F. B. Wilm, T. Eder, C. Mück-Lichtenfeld, P. Mehlmann, M. Wünsche, F. Buß and F. Dielmann, *Green Chem.*, 2019, **21**, 640–648.
- 54 J. Garnier, A. R. Kennedy, L. E. A. Berlouis, A. T. Turner and J. A. Murphy, *Beilstein J. Org. Chem.*, 2010, **6**, 73.
- 55 P. Pyykkö and M. Atsumi, *Chem. – Eur. J.*, 2009, **15**, 186–197.
- 56 P. Pyykkö and M. Atsumi, *Chem. – Eur. J.*, 2009, **15**, 12770–12779.
- 57 J. L. Doran, B. Hon and K. R. Leopold, *J. Mol. Struct.*, 2012, **1019**, 191–195.
- 58 K. D. Vogiatzis, A. Mavrandonakis, W. Klopfer and G. E. Froudakis, *ChemPhysChem*, 2009, **10**, 374–383.
- 59 S. Y. Han, I. Chu, J. H. Kim, J. K. Song and S. K. Kim, *J. Chem. Phys.*, 2000, **113**, 596–601.
- 60 M. Z. Kamrath, R. A. Relph and M. A. Johnson, *J. Am. Chem. Soc.*, 2010, **132**, 15508–15511.
- 61 D. V. Vasilyev and P. J. Dyson, *ACS Catal.*, 2021, **11**, 1392–1405.
- 62 J. K. Mannisto, L. Pavlovic, T. Tiainen, M. Nieger, A. Sahari, K. H. Hopmann and T. Repo, *Catal. Sci. Technol.*, 2021, **11**, 6877–6886.
- 63 X. Yang, R. J. Rees, W. Conway, G. Puxty, Q. Yang and D. A. Winkler, *Chem. Rev.*, 2017, **117**, 9524–9593.
- 64 L. J. Murphy, K. N. Robertson, R. A. Kemp, H. M. Tuononen and J. A. C. Clyburne, *Chem. Commun.*, 2015, **51**, 3942–3956.
- 65 H. Zhou and X. Lu, *Sci. China: Chem.*, 2017, **60**, 904–911.
- 66 P. Sreejyothi and S. K. Mandal, *Chem. Sci.*, 2020, **11**, 10571–10593.
- 67 J. W. Keller, *J. Phys. Chem. A*, 2015, **119**, 10390–10398.
- 68 K. Huynh, E. Rivard, A. J. Lough and I. Manners, *Chem. – Eur. J.*, 2007, **13**, 3431–3440.
- 69 N. Patel, M. Arfeen, R. Sood, S. Khullar, A. K. Chakraborti, S. K. Mandal and P. V. Bharatam, *Chem. – Eur. J.*, 2018, **24**, 6418–6425.



- 70 S. Coffie, J. M. Hogg, L. Cailler, A. Ferrer-Ugalde, R. W. Murphy, J. D. Holbrey, F. Coleman and M. Swadźba-Kwaśny, *Angew. Chem., Int. Ed.*, 2015, **54**, 14970–14973.
- 71 P. H. Clippard, J. C. Hanson and R. C. Taylor, *J. Cryst. Mol. Struct.*, 1971, **1**, 363–371.
- 72 H. V. Huynh, Y. Han, R. Jothibasur and J. An Yang, *Organometallics*, 2009, **28**, 5395–5404.
- 73 Q. Teng and H. V. Huynh, *Dalton Trans.*, 2017, **46**, 614–627.
- 74 Y. Han, H. V. Huynh and G. K. Tan, *Organometallics*, 2007, **26**, 6447–6452.
- 75 Q. Teng, P. S. Ng, J. N. Leung and H. V. Huynh, *Chem. – Eur. J.*, 2019, **25**, 13956–13963.
- 76 D. G. Gusev, *Organometallics*, 2009, **28**, 6458–6461.
- 77 E. Larionov and H. Zipse, *Wiley Interdiscip. Rev.: Comput. Mol. Sci.*, 2011, **1**, 601–619.
- 78 A. Ruiz, P. Rocca, F. Marsais, A. Godard and G. Quéguiner, *Tetrahedron Lett.*, 1997, **38**, 6205–6208.
- 79 A. R. Katritzky and S. S. Thind, *J. Chem. Soc., Perkin Trans. 1*, 1980, 1895.
- 80 L. W. Deady and W. L. Finlayson, *Synth. Commun.*, 1980, **10**, 947–950.
- 81 L. W. Deady and O. L. Korytsky, *Tetrahedron Lett.*, 1979, **20**, 451–452.
- 82 C. Yin, K. Zhong, W. Li, X. Yang, R. Sun, C. Zhang, X. Zheng, M. Yuan, R. Li, Y. Lan, H. Fu and H. Chen, *Adv. Synth. Catal.*, 2018, **360**, 3990–3998.

